

Edward Lisowski (lisowski@mech.pk.edu.pl)

Stanisław Okoński

Wojciech Czyżycki

Institute of Applied Informatics, Faculty of Mechanical Engineering, Cracow University of Technology

## SIMULATION STUDIES ON RING UPSETTING USING THE ABAQUS SOFTWARE

### BADANIA SYMULACYJNE SPĘCZANIA PIERŚCIENI W PROGRAMIE ABAQUS

#### Abstract

In this paper, a simulation and an experimental analysis of upsetting a cold ring placed between two rigid plates were conducted. When designing a new process, it is preferable to carry out the simulation studies using FEM, which allow for the prediction of the course and proper selection of process conditions. Due to the complexity of phenomena that occur during plastic formation, it is essential to have a good description of contact phenomena and properties of material in the plastic state. The computer simulation was performed for a specific material – a thick plate of hot-rolled carbon steel with fixed initial dimensions of rings and different values of the coefficient of friction.

**Keywords:** upsetting, friction, FEM simulation

#### Streszczenie

W niniejszym artykule przeprowadzono analizę MES spęczania na zimno pierścienia umieszczonego pomiędzy dwoma sztywnymi płytami. Symulację komputerową przeprowadzono dla konkretnego materiału – blachy grubej walcowanej na gorąco ze stali niskowęglowej przy ustalonych wymiarach początkowych pierścieni i różnych wartościach współczynników tarcia. Krzywą wzmocnienia wyznaczono w badaniach własnych. Obliczone wymiary pierścieni oraz wartości sił spęczania porównano z wynikami doświadczalnymi. Wyraźnie widać silny wpływ warunków tarcia na niejednorodność odkształceń, a zwłaszcza na charakter zmian średnic wewnętrznych. Wykonano badania doświadczalne spęczania z użyciem gładkich i chropowatych kowadeł na sucho i ze smarem, zmieniając w ten sposób warunki tarcia na powierzchniach kontaktowych.

**Słowa kluczowe:** spęczenie, tarcie, analiza MES

## 1. Introduction

While designing a new process, it is preferable to carry out simulation studies. They allow for the prediction of the process and help to check the proper selection of process conditions. There are many commercial programs which allow us to carry out this type of study. Essa et al. [4] used Ansys, which is general finite element method software, for the examination of the behavior of bi-metallic components during the cold upsetting process. Luo et al. [12] simulated sheet metal flanging and upsetting process by means of the MSC.Marc software. There is more special software such as e.g. eta/DYNAFORM used for modelling of the stamping process by Hojny et al. [7]. Due to the complexity of phenomena that occur during plastic formation, it is essential to have a good description of the contact phenomena and properties of material in the plastic state.

The problem regarding computer modeling of metal forming processes has been a subject of many scientific works. The article by Behrens and Schafstall [1] is dedicated to 2D and 3D modeling of forging processes considering friction forces. Another author, Lacki [11] discusses the use of various models of friction in computer simulations. The other work by the same author Lacki [10] concerns the modeling process of upsetting. Khoei et al. [8] present a calculation algorithm for modeling friction in processes of compressible material forming.

Coulomb friction law can be successfully used in the analysis of a metal forming process provided that the assumed values of the friction coefficient correspond to the actual conditions. Gieżyńska [5] draws attention to the diversity of phenomena occurring at the contact surfaces under high unit pressures and presents a number of experimental methods which allow for setting coefficients of friction in metal forming processes. In the methods, also discussed by Morawiecki et al. [14], independent measurements of the tangential force ( $T$ ) and the normal force ( $N$ ) to the contact surface are utilized, or the  $T/N = \mu$  ratio is directly determined (i.e. in the rolling process, where  $\mu = \tan(\alpha)$  is a limit value of a gripping angle). Methods of experimental research of friction in elastic and plastic areas of the contact surface are described by Tajdari and Javadi [17].

The occurrence of stresses of different values on contact surfaces, caused by friction, significantly affects the shape of the deformed object. Therefore, coefficients of friction can also be set by studying changes in the dimensions of samples deformed under various conditions. The essence of the method involves the use of the boundary problem solution in the equations of the theory of plasticity which describe the change of sample's dimensions with fixed initial dimensions for assumed values of the friction coefficient. The theoretical relationship between the strain and friction conditions can be represented in the following general form:

$$F_i(e_1, e_2) = 0 \text{ for } \mu = \text{const} \quad (1)$$

where independent variables  $e_1$  and  $e_2$  characterize the deformation state. Deformations or the final dimensions of samples can be taken as the  $e_1$  and  $e_2$  variables (from the fixed initial dimensions).

Male and Cockroft [13] inspired by Kunogi's idea [9] provided a suitable theoretical solution and developed a nomogram showing functions (1) for upsetting rings of fixed dimensional proportions  $D_0 : d_0 : h_0 = 2:1:0.7$  (Fig. 1), by assuming that:

$$e_1 = \varepsilon_h = \frac{h_0 - h_1}{h_1}, \quad (2)$$

$$e_2 = \frac{d_0}{d_1}, \quad (3)$$

The friction coefficient is determined by measuring the inner diameter  $d$  and height of the ring after upsetting; see Burgdorf [2]. The nomogram developed by A.T. Male, and M.G. Cockford is cited by many authors, including Gieżyńska [5], Sofuoğlu and Gedikli [16]. Further studies of this method were conducted among others by Wang and Lenard [18] and also Pawelski et al. [15]. It should be noted that, using current advancement of computational methods (FEM), nomograms for determining friction coefficients can be built on the basis of deformation of samples which are not ring-shaped.

A new method (ODBET) developed by Sofuoğlu and Gedikli [16] is worth mentioning. It consists of pressing cylindrical samples on the lower anvil, while the top anvil has an edge-rounded hole. Therefore, a counter extrusion of material into the hole of the upper anvil occurs. The height of portion of the sample squeezed into the hole, as well as other dimensions depend on the coefficient of friction at the contact surfaces. The authors developed appropriate nomograms using ANSYS software. It should be mentioned that earlier a similar method had been proposed by Herold [6], wherein the friction coefficient was determined based on the height of the rectangular portion of the sample formed by extrusion into the slot of the upper anvil.

As it turned out, the main advantage of the method of upsetting rings (in addition to the simplicity of its implementation) is strong influence of friction on the  $e_1$  and  $e_2$  variables, making it possible to detect even small changes of the friction coefficient. The nomogram developed by Male and Cockroft [13] is universal, independent of the type of material and thermodynamic conditions of deformation process. Because the characteristics of the material and thermodynamic conditions have a significant influence on the deformation, in this article it is proposed that the  $F_i$  functions are determined individually for different materials, initial ratios of ring dimensions and strain conditions.

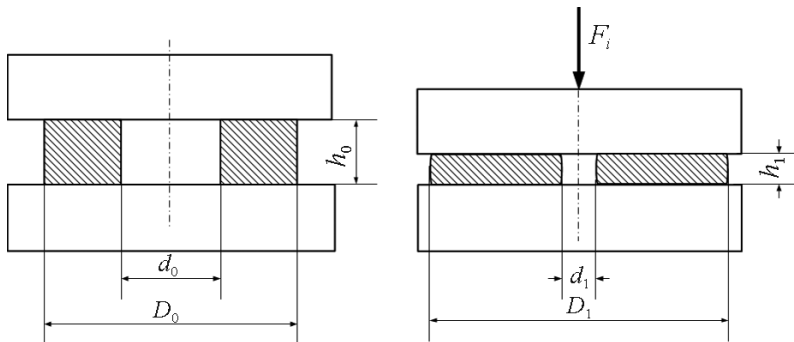


Fig. 1. Scheme of the ring before and after upsetting (on the right)

## 2. Material model and conditions of deformation

Rings made of the S235JR steel with dimensions:  $D_0 = 20$  mm,  $d_0 = 10$  mm and  $h_0 = 8$  mm were used in the simulations. It was assumed that the materials were homogeneous, isotropic, elastic-plastic, with the isotropic hardening and incompressible in terms of plastic. Cold deformation is carried out under isothermal and quasi-static conditions. With these assumptions, the following Huber-Mises condition is valid:

$$3J_2' - \sigma_p^2(\bar{\varepsilon}^{pl}) = 0, \quad (4)$$

as well as the constitutive equation of Prandtl-Reuss:

$$d\varepsilon_{ij} = \frac{1+\nu}{E} \left( d\sigma_{ij} - \frac{\nu}{1+\nu} d\sigma_{kk} \delta_{ij} \right) + \frac{3d\bar{\varepsilon}^{pl}}{2\sigma_p \bar{\varepsilon}} S_{ij}, \quad (5)$$

where:

$J_2'$  – second invariant of the deviatoric stress tensor  $\mathbf{S}$ :

$$J_2' = \frac{1}{2} \mathbf{S} : \mathbf{S}, \quad (6)$$

$$\mathbf{S} = \sigma - \frac{1}{3} \sigma : \mathbf{I}, \quad (7)$$

where:

$\nu$  – Poisson's ratio,

$E$  – Young's modulus,

$\bar{\varepsilon}^{pl}$  – equivalent plastic a plastic strain:

$$\bar{\varepsilon}^{pl} = \int \sqrt{\left( \frac{2}{3} d\varepsilon^{pl} : d\varepsilon^{pl} \right)}. \quad (8)$$

## 3. Experimental identification of parameters describing the material

Parameters describing the material were defined in the uniaxial tension and compression tests. The values of equivalent strain and yield stress in the tensile tests were determined by the following formulas:

$$\bar{\varepsilon}^{pl} = \ln(1 + \varepsilon_{\text{nom}}) - \frac{\sigma_{tr}}{E}, \quad (9)$$

$$\sigma_p = \sigma_{tr} = \frac{P}{F_0} (1 + \varepsilon_{\text{nom}}), \quad (10)$$

where:

$$\varepsilon_{\text{nom}} = \frac{\Delta l}{l_0}, \quad (11)$$

$l_0, F_0$  – respectively: length and area of measuring section,  
 $P$  – force,  
 $s_{tr}$  – actual stress,  
 $e_{\text{nom}}$  – relative strain.

Compression tests were used for large deformations ( $\varepsilon$ ). In these tests, conditions similar to the absence of friction were provided. Cylindrical samples with dimensions  $d_0 = h_0 = 7$  mm with greased recesses in the faces and polished anvils were used. The yield stress was determined by introducing an amendment which takes into account the impact of low friction ( $\mu \approx 0.5$ ) on the surface of the anvils, according to Morawiecki et al. [14]:

$$\sigma_{tr} = \frac{4P}{\pi d^2} = \frac{2\sigma_p h^2}{\mu^2 d^2} \left[ \exp\left(\frac{\mu d}{h}\right) - \frac{\mu d}{h} - 1 \right]. \quad (12)$$

The equivalent strain was calculated from the following formula:

$$\varepsilon^{pl} = 2 \ln \frac{d}{d_0}. \quad (13)$$

In order to determine the elastic constant, measurements of a low longitudinal and transverse strain of the tensile were carried out. Electro strain gauges 1XY91-3/120 glued on the measuring sections of the samples were used for this purpose. Elastic constants were as follows: Poisson's ratio  $\nu = 0.28$ , Young's modulus  $E = 2.09 \cdot 10^5$  MPa.

Fig. 2 shows the hardening curve used in the calculations approximated by the function:

$$\sigma_p = 256 + 572\varepsilon^{-0.629}. \quad (14)$$

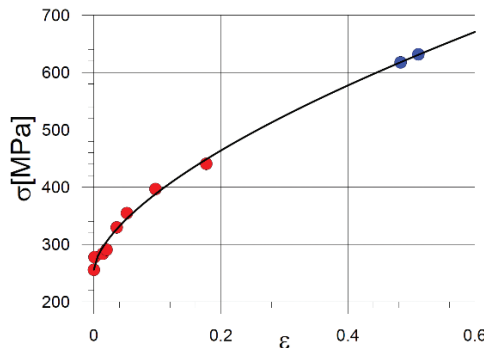


Fig. 2. The hardening curve determined for calculations (red points denote tensile measurements, blue points – compression measurements)

#### 4. FEM analysis

A FEM analysis of the ring upset was carried out in the ABAQUS software [3]. The ring, geometrical models of fixed anvil and movable anvil were built for this purpose. The elements have been built as separate parts of the assembly. When depositing the parts to the FEM analysis, it was assumed that the fixed anvil is rigid, movable anvil is also rigid and can move only vertically. The ring model was built as a deformable axially symmetric (Fig. 3). Ring dimensions were set as follows:  $D_0 = 20$  mm,  $d_0 = 10$  mm,  $h_0 = 8$  mm. The FEM model of the ring was constructed by imposing the following conditions: *max size* – 0.2 mm, *max deviation factor* – 0.1. The interaction between the walls of the ring and anvils was defined as a *type of contact*, assuming a constant coefficient of friction  $\mu$ . In the normal direction, the pressure overclosure parameter was assumed as *Hard Contact*, *constraint enforcement* as *penalty* and *contact stiffness* as *linear*.

Fig. 4 shows the results of the ring deformation obtained for displacement of the anvil equal to 3 mm and Fig. 5 – for a 5 mm displacement, with the friction coefficient  $\mu = 0.07$ . As can be seen from the comparison of the drawings, the level of deformation significantly affects the cross-sectional shape of the ring. A similar phenomenon can also be observed for the results obtained for the coefficient of friction of 0.12 and 0.577 (Figs. 6–9). The simulation results confirm that the friction coefficient value has a particular influence on the inner diameter of the ring. At low values of the friction coefficient, inner diameters of the ring are subject to a small change. However, if the value of friction coefficient is above 0.5, the value of an inner diameter decreases rapidly.

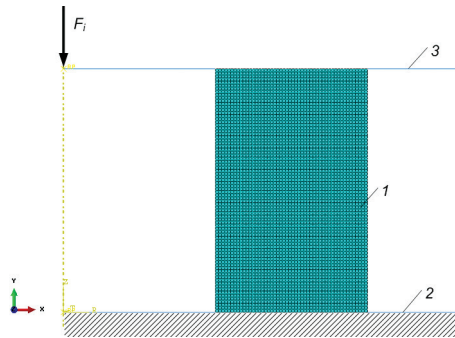


Fig. 3. Model mesh: 1 – deformable ring, 2, 3 – rigid plate; *max mesh size* – 0.2 mm

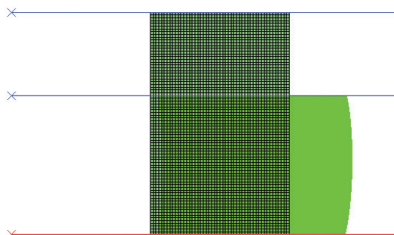


Fig. 4. Deformation of the ring for  $\mu = 0.07$ ,  $h_1 = 5$  mm

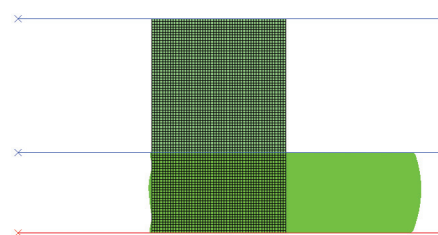


Fig. 5. Deformation of the ring for  $\mu = 0.07$ ,  $h_1 = 3$  mm

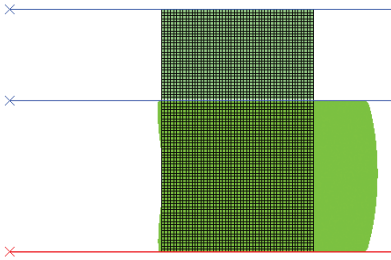


Fig. 6. Deformation of the ring for  $\mu = 0.12$ ,  $h_1 = 5 \text{ mm}$

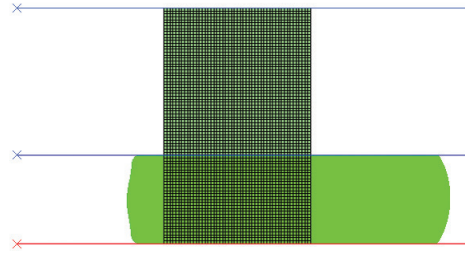


Fig. 7. Deformation of the ring for  $\mu = 0.12$ ,  $h_1 = 3 \text{ mm}$

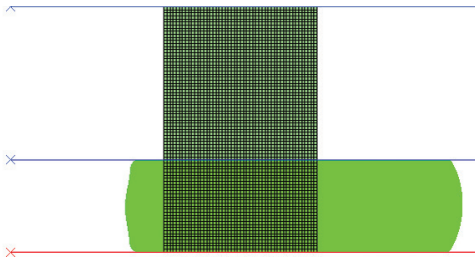


Fig. 8. Deformation of the ring for  $\mu = 0.577$ ,  $h_1 = 5 \text{ mm}$

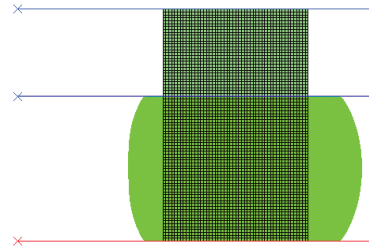


Fig. 9. Deformation of the ring for  $\mu = 0.577$ ,  $h_1 = 3 \text{ mm}$

In Figs. 10–15, distributions of equivalent plastic strain are shown (PEEQ) according to formula (9). As it can be clearly seen, there is a strong heterogeneity of deformation at high strain values and coefficients of friction (Fig. 15,  $\mu = 0.577$ ). The friction coefficient value  $\mu = 0.577$  is the value at which stress reaches the value of  $\sigma_p / \sqrt{3}$  and the material is adhered to the anvil.

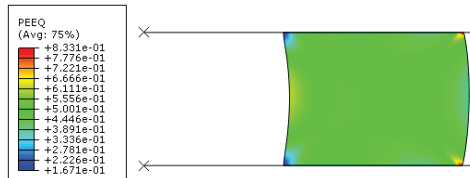


Fig. 10. Distribution of equivalent plastic strain (PEEQ);  $\mu = 0.07$ ,  $h_1 = 5 \text{ mm}$

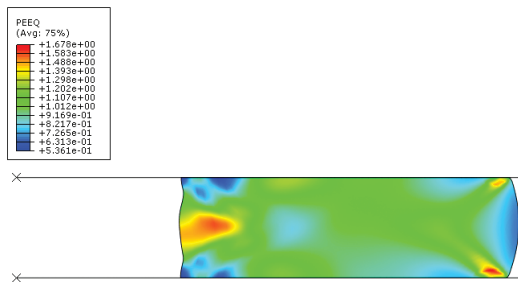


Fig. 11. Distribution of equivalent plastic strain (PEEQ);  $\mu = 0.07$ ,  $h_1 = 3 \text{ mm}$

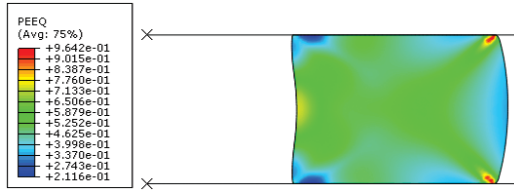


Fig. 12. Distribution of equivalent plastic strain (PEEQ);  $\mu = 0.12, h_1 = 5 \text{ mm}$

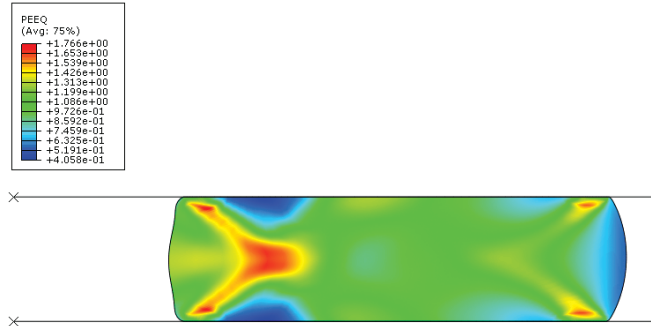


Fig. 13. Distribution of equivalent plastic strain (PEEQ);  $\mu = 0.12, h_1 = 3 \text{ mm}$

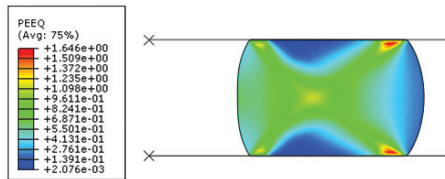


Fig. 14. Distribution of equivalent plastic strain (PEEQ);  $\mu = 0.0577, h_1 = 5 \text{ mm}$

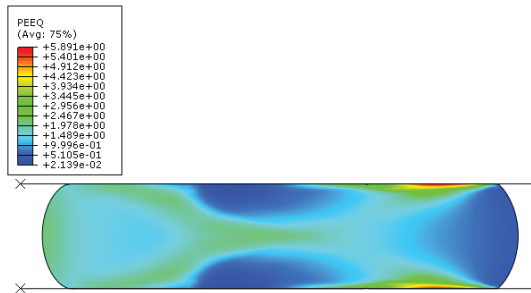


Fig. 15. Distribution of equivalent plastic strain (PEEQ);  $\mu = 0.577, h_1 = 3 \text{ mm}$

## 5. Comparison of calculation results and experiments

In order to verify the results of calculations performed in the ABAQUS software, experimental studies on the rings with identical dimensions as in the FEM analysis were carried out. The upsetting process was performed on the anvil with properly prepared surfaces and applied lubrication, which allowed for obtaining different coefficients of friction.



## 5.1. Changes of the outer diameter

Fig. 16 shows the relative changes of the internal diameter of the ring as a function of the height reduction computed using the FEM analysis (solid line). On the graph, experimental points marked by different colours were also plotted. The measurement points corresponding to upsetting on the smooth anvils without lubricant (blue marks) are best suited to the curve corresponding to the friction coefficient of 0.12. Red points – which correspond to upsetting on the smooth lubricated anvils – best fit to the curve corresponding to the friction coefficient  $\mu = 0.07$ . As controls, upsetting on the anvils grooved was also carried out (recommended by the CIRP, ICFG and INOP). The results of measurements (green marks) lie on the curve corresponding to the maximum coefficient of friction  $\mu = 0.577$ .

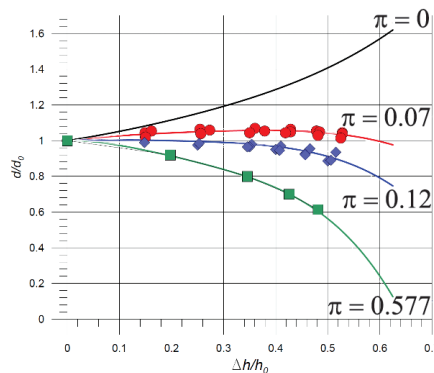


Fig. 16. Results of measurements of the rings' internal diameters after upsetting (red marks – anvils without lubrication, blue marks – anvils lubricated) on the background of the lines for fixed values of the friction coefficients

## 5.2. Shape of the samples after upsetting

To analyze the cross-sectional shape of the ring after upsetting, three characteristic samples with height reduced to  $\Delta h = h_0 = 3/8$  and the coefficients of friction respectively 0.07, 0.12 and 0.577 have been chosen. Appearance of the cross section of the cut sample is shown in Figs. 17a–19a. For comparison, in Figs. 17b–19b, sections obtained by the FEM analysis are presented. It is apparent from the drawings that there is a strong resemblance to the actual shape obtained in the FEM analysis.

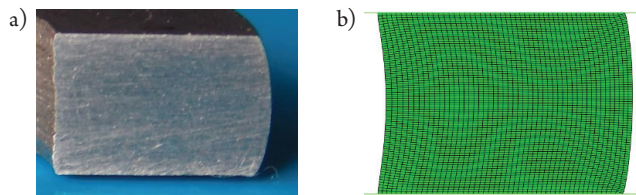


Fig. 17. Comparison of the shape for  $\mu = 0.07$ ,  $h_1 = 5$  mm: a) the actual cross-section, b) the shape obtained from the FEM analysis

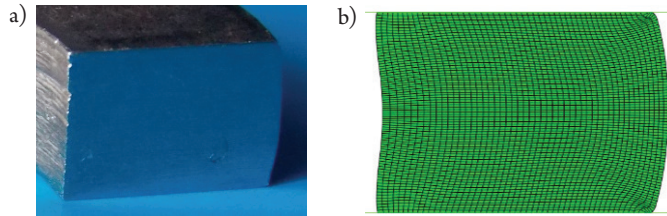


Fig. 18. Comparison of the shape for  $\mu = 0.12$ ,  $h_1 = 5$  mm: a) the actual cross-section, b) the shape obtained from the FEM analysis

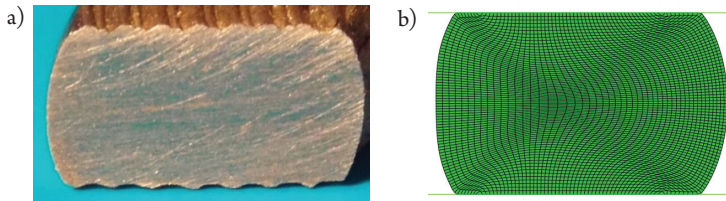


Fig. 19. Comparison of the shape for  $\mu = 0.577$ ,  $h_1 = 5$  mm: a) the actual cross-section, b) the shape obtained from the FEM analysis

In order to compare the dimensions of the cross sections obtained in the FEM analysis with the actual measuring, 12 evenly spaced points have been selected along the Y-axis as in Fig. 20. The values of the X-coordinate obtained in the FEM analysis have very similar values in many points. The largest differences in the X coordinate do not exceed 5%.

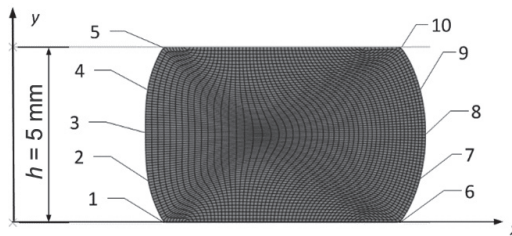


Fig. 20. Selected measuring points of the shape coordinates after upsetting the sample

## 6. Summary

The article presents the results of a computer simulation of a ring upsetting process using FEM. ABAQUS software was used. The calculations were performed for fixed dimensions of the rings and particular material for which the hardening curve was determined experimentally. Thus, relationships between different values of friction coefficients and such parameters as inner diameter, distribution of equivalent strain and upsetting force were determined. It can be clearly seen that there is a strong influence of friction conditions on the heterogeneity of deformation (Figs. 10–15) and, in particular, on the nature of changes of internal diameters (Figs. 4–9). Experimental upsetting studies were performed using smooth and rough anvils

– with and without lubrication – which caused changes in friction conditions on the contact surfaces. There was a good correlation between the actual and FEM – calculated shapes of the deformed rings (Figs. 17–19). In addition, the resulting dimensions of upsetting rings have been shown in the background of theoretical relations of diameters  $d = d_0$  depending on the height changes  $\Delta_h = h_0$  (Fig. 16). The experimental points fit well with their corresponding theoretical curves, which confirms the possibility of using the presented method of ring upsetting to determine friction coefficients' values.

## References

- [1] Behrens A., Schafstall H., *2D and 3D simulation of complex multistage forging processes by use of adaptive friction coefficient*, Journal of Materials Processing Technology, 80–81, 1998, 298–303.
- [2] Burgdorf M., *Über die Ermittlung des Reibwertes für verfahren der Massivumformung durch den Ringstauchversuch Ind.*, Anz. Steel Research, 89, 1967.
- [3] Dassault Systemes, Abaqus Documentation and User Manual, Version 6.12, 2012.
- [4] Essa K., Kacmarcik I., Hartley P., Plancak M., Vilotic D., *Upsetting of bi-metallic ring billets*, Journal of Materials Processing Technology, 212, 2012, 817–824.
- [5] Gieżyńska M., *Tarcie, zużycie i smarowanie w obróbce plastycznej metali*, WNT, Warszawa 1992.
- [6] Herold K., *Steigversuch an Flachproben-Ein neues Verfahren zur Ermittlung des Reibungskoeffizienten bei Umformvorgängen*, Fertigungstechnik und Betrieben, 2, 1968.
- [7] Hojny M., Głowacki M., Opaliński A., Woźniak D., *Computer aided design of stamping process technology using the eta/Dynaform 5.8 system*, Technical Transactions, vol. 4-M/2011, Cracow University of Technology Press.
- [8] Khoei A., Biabanaki S.O.R., Vafa A.R., Yadegaran I., Keshavarz S.H., *A new computational algorithm for contact friction modeling of large plastic deformation in powder compaction processes*, International Journal of Solids and Structures, 46, 2009.
- [9] Kunogi M., *A new method of cold extrusion*, J. Sci. Res. Inst., 50, 1956, 215–246.
- [10] Lacki P., *Simulation of friction in upsetting process*, International Journal of Applied Mechanics and Engineering, 9, 2004, 247–253.
- [11] Lacki P., *Zastosowanie wybranych modeli tarcia w numerycznej analizie procesów obróbki plastycznej*, Konferencja nt. „Informatyka w technologii metali” 11–14 stycznia 2004, Wyd. Nauk. AKAPIT, Kraków 2004.
- [12] Luo J., Wang X., Guo M., Xia J., *Precision research in sheet metal flanging and upset extruding*, Materials Research Innovations, 15, 2011, 439–442.
- [13] Male A.T., Cockroft M.G., *A method for the determination of the coefficient of friction of metals under conditions of bulk plastic deformation*, Journal of the Institute of Metals, 93, 1964, 38–46.
- [14] Morawiecki M., Sadok L., Wosiek E., *Przeróbka plastyczna. Podstawy teoretyczne*, Wyd. Śląsk, Katowice 1986.

- [15] Pawelski O., Rasp W., Hoerster C., *The ring compression test as simulation test for the investigation of friction in hot metal forming*, Steel Research, 60, 1989.
- [16] Sofuoglu H., Gedikli H., *Determination of friction coefficient encountered in large deformation processes*, Tribology International 35, 2002, 27–34; doi:[http://dx.doi.org/10.1016/S0301-679X\(01\)00076-7](http://dx.doi.org/10.1016/S0301-679X(01)00076-7).
- [17] Tajdari M., Javadi M., *A new experimental procedure of evaluating the friction coefficient in elastic and plastic regions*, Journal of Materials Processing Technology 177, 2006, 247–250.
- [18] Wang F., Lenard J.G., *An experimental study of interfacial friction hot ring compression*, Journal of Engineering Materials and Technology, 114, 1992, 13–18.